



Published in final edited form as:

Brain Behav Immun. 2015 August ; 48: 139–146. doi:10.1016/j.bbi.2015.03.009.

Aberrant neuron morphology in a nonhuman primate model of maternal immune activation

Ruth K. Weir^{1,*}, Reihaneh Forghany¹, Stephen E.P. Smith², Paul H. Patterson^{3,†}, A. Kimberly McAllister⁴, Cynthia M. Schumann^{1,#}, and Melissa D. Bauman^{1,#}

¹The Department of Psychiatry and MIND Institute, University of California, Davis, CA, 95817, USA

²Dept. of Immunology, Mayo Clinic College of Medicine, Rochester, MN, 55905, USA

³California Institute of Technology, Pasadena, CA 91125, USA

⁴Center for Neuroscience, University of California Davis, Davis, CA, 95618 USA

Abstract

Maternal infection during pregnancy increases the risk for neurodevelopmental disorders in offspring. Rodent models have played a critical role in establishing maternal immune activation (MIA) as a causal factor for altered brain and behavioral development in offspring. We recently extended these findings to a species more closely related to humans by demonstrating that rhesus monkeys (*Macaca mulatta*) prenatally exposed to MIA also develop abnormal behaviors. Here, for the first time, we present initial evidence of underlying brain pathology in this novel nonhuman primate MIA model. Pregnant rhesus monkeys were injected with a modified form of the viral mimic polyI:C (poly ICLC) or saline at the end of the first trimester. Brain tissue was collected from the offspring at 3.5 years and blocks of dorsolateral prefrontal cortex (BA46) were used to analyze neuronal dendritic morphology and spine density using the Golgi-Cox impregnation method. For each case, 10 layer III pyramidal cells were traced in their entirety, including all apical, oblique and basal dendrites, and their spines. We further analyzed somal size and apical dendrite trunk morphology in 30 cells per case over a 30µm section located 100±10µm from the soma. Compared to controls, apical dendrites of MIA-treated offspring were smaller in diameter and exhibited a greater number of oblique dendrites. These data provide the first evidence that prenatal exposure to MIA alters dendritic morphology in a nonhuman primate MIA model, which may have profound implications for revealing the underlying neuropathology of neurodevelopmental disorders related to maternal infection.

*Corresponding author (for editorial process), Ruth Weir Ph.D. Department of Psychiatry & Behavioral Sciences, University of California, Davis, CA, USA ; The MIND Institute, University of California, Davis, 2825 50th Street, Sacramento, CA 95817, USA. rkweir@ucdavis.edu 916-703-0341. *Corresponding author (for publication), Melissa Bauman Ph.D. Department of Psychiatry & Behavioral Sciences, University of California, Davis, CA, USA ; The MIND Institute, University of California, Davis, 2825 50th Street, Sacramento, CA 95817, USA. mdbauman@ucdavis.edu 916-703-0377.

#Co-senior author,

†Deceased

Keywords

polyIC; nonhuman primate; pyramidal neuron morphology; neurodevelopment; schizophrenia; autism; IL-6

Introduction

Exposure to infection during pregnancy increases the risk of offspring developing neuropsychiatric disorders such as autism spectrum disorder (ASD) and schizophrenia (Abdallah et al., 2012; Atladóttir et al., 2012, 2010; Brown et al., 2004; Lee et al., 2014; Mednick et al., 1988; Sørensen et al., 2009). The diversity of infections associated with altered neurodevelopment suggests that the mother's immune response, rather than a specific pathogen, underlies changes in fetal brain development. In support of this, maternal immune activation (MIA) in pregnant rodents yields offspring with behavioral abnormalities and brain pathology that parallel features of human neurodevelopmental disorders (Patterson, 2009). Aberrant development of rodent offspring can be induced by exposing the pregnant dam to influenza (Fatemi et al., 2008; Shi et al., 2003), the bacterial endotoxin lipopolysaccharide (LPS) (Baharnoori et al., 2009; Fortier et al., 2007) or the double stranded RNA viral mimic polyinosinic:polycytidylic acid (polyI:C) (Malkova et al., 2012; Piontkewitz et al., 2012; Shi et al., 2003; Zuckerman and Weiner, 2005, 2003).

Rhesus monkey (*Macaca mulatta*) models of human disorders provide an intermediate step between rodent models and clinical populations given the higher level of homology between humans and nonhuman primates in behavior, anatomy, and physiology (Watson and Platt, 2012). Previous nonhuman primate models have documented neurobehavioral abnormalities in macaque offspring following third trimester exposure to influenza or the bacterial endotoxin lipopolysaccharide (LPS) (Short et al., 2010; Willette et al., 2011). However, the effects of MIA at earlier gestational time points have not been explored in the nonhuman primate. We developed a novel, rhesus monkey MIA model using a modified form of poly I:C (poly ICLC), a double-stranded RNA that induces a transient innate inflammatory response in the primate immune system (Caskey et al., 2011; Levy et al., 1975). An initial cohort of animals was produced to establish dosing protocols, followed by a larger cohort that underwent comprehensive behavioral phenotyping from birth to four years of age. The MIA-treated offspring in the larger cohort demonstrated abnormal repetitive behaviors, altered vocal communication and atypical social interactions (Bauman et al., 2014). Non-invasive eye-tracking studies later revealed that the MIA-treated juvenile offspring fail to attend to salient social cues (Machado et al., 2014). The behavioral pathology in the monkey poly ICLC model extends the findings from rodent MIA models to more human-like behaviors resembling those in both ASD and SZ.

An essential next step is to determine if MIA-exposed macaque offspring also demonstrate brain neuropathology that parallels these human disorders. While behavioral studies were being carried out on the larger cohort, we initiated the neuropathological examination of brain tissue from the initial polyICLC dosing cohort. Offspring from this initial cohort were born to dams injected with polyICLC at six time points at the end of the first trimester to

evaluate the maternal immune response (N=4) or born to saline injected controls (N=4). Brain tissue was collected at 3.5 years of age and stained with a modified Golgi-Cox technique (Glaser and Van der Loos, 1981). We have focused our initial studies of neuronal morphology on the dorsolateral prefrontal cortex (DLPC; Brodmann Area 46), an area known to show changes in layer III pyramidal neuron morphology in post-mortem populations of SZ patients (Glantz and Lewis, 2000; Glausier and Lewis, 2013; Kolluri et al., 2005; Pierri et al., 2001). The DLPFC is well-developed in primates and is a good candidate area to identify potential aberrant neuronal dendritic morphology in MIA-exposed offspring in a brain region implicated in human neuropsychiatric disease.

Materials and Methods

All experimental procedures were developed in collaboration with the veterinary, animal husbandry, and environmental enrichment staff at the California National Primate Research Center (CNPRC) and approved by the University of California, Davis Institutional Animal Care and Use Committee. All attempts were made (in terms of social housing, enriched diet, use of positive reinforcement strategies, and minimizing the duration of daily training/testing sessions) to promote the psychological well-being of the animals that participated in this research.

Subjects

Eight pregnant rhesus monkeys were selected from the timed-mating program at the California National Primate Research Centre and randomly assigned to receive saline control injections (n=4) or a modified form of the viral mimic polyI:C (polyinosinic:cytidylic acid, stabilized with poly-L-lysine (polyICLC)) (Oncovir Inc., Washington D.C.) (n=4). PolyICLC is resistant to endogenous RNase activity present in primate blood that breaks down polyIC (de Clercq, 1979; Nordlund et al., 1970). Pregnancy was confirmed at approximately 20 days of gestation via ultrasound. Willingness to present an arm for intravenous injection while being temporarily restrained (less than 1min) was assessed at gestational day 30. To minimize stress, only animals that readily complied were included in the study.

Maternal PolyICLC administration

Pregnant dams received six intravenous injections of polyICLC or saline on gestational days 43, 44, 46, 47, 49 and 50 of pregnancy (at the end of the first trimester). The dose of polyIC utilized in rodent MIA models generally ranges from 4–20mg/kg (Boksa, 2010). Lower doses were initially evaluated in the nonhuman primate model to establish parameters for stimulating a maternal immune response while minimizing spontaneous abortion. Three low doses were evaluated in this study: 0.25, 0.5 and 1 mg/kg (n=1,2,1 respectively). The control group received saline injections to account for any differences that may arise from stress of receiving injections in pregnancy. Pregnancies of both MIA and control animals were monitored via ultrasound 24–48 hours following the final polyICLC or saline injection, and again at approximately GD 100 and 150. Note that for the larger cohort of MIA-treated offspring utilized in the behavioral studies (Bauman et al., 2014; Machado et al., 2014) the

lowest dose of polyICLC was used (0.25mg/kg) and the number of polyICLC injections was reduced from six to three.

Interleukin-6 analysis

Blood was drawn 24–48 hours prior to the initial polyICLC injection for baseline analysis, and then again three hours after the first and last injections were administered (GD 43 and 50). A final sample was collected approximately 5-days after polyICLC injections as a second baseline measure (Table 1). Blood was separated and serum was diluted with PBS/ 0.2%BSA to fall into the linear range of a primate specific IL-6 ELISA assay (Cell Sciences, Canton, MA).

Offspring and behavioral scoring

The offspring (6males, 2 females) were raised with their mothers and provided access to peers to facilitate species typical social development. While comprehensive behavioral phenotyping was not carried out on the initial dosing cohort, general health and development were monitored and the offspring were periodically screened for maladaptive behaviors, such as repetitive behaviors. Quantitative behavioral data were collected when the offspring were weaned from their mothers at six months of age. Trained observers, who were blind to the assigned experimental conditions, conducted 18 home cage observations (9 morning and 9 afternoon sessions) in a pre-determined pseudo-random order for six ten-second periods. At the onset of each observation, the observer approached to one meter in front of the home cage and recorded behaviors using a one-zero sampling method. Any behavior occurring within the ten-second observation received a score of “1” (even if the behavior was repeated), whereas behaviors that were not observed during the trial received a score of “0”. Behaviors included a subset of the standard rhesus monkey developmental ethogram (Bauman et al., 2014), focusing specifically on maladaptive motor stereotypies and self-directed behaviors.

Histological evaluation of tissue

Animals were perfused at 3.5 years of age and the brains placed in 10% formalin prior to processing less than a week later. The left hemisphere was retained for the current study, while the right hemisphere was frozen and retained for future studies. Left hemisphere frontal lobe blocks were wrapped in gauze and placed in Golgi-Cox solution (working concentrations: 1% potassium dichromate, 1% mercuric chloride and 0.83% potassium chromate) for 12 weeks (Das et al., 2013; Rosoklija et al., 2003). Tissue blocks were then dehydrated in alcohols, embedded in parlodion, and cut on a sliding microtome in to 150µm thick sections (Microm HM440E). Sections were developed in ammonium hydroxide for 10 minutes followed by 5 minutes in Kodak film fixer. Sections were then washed in water and dehydrated in graded concentration of ethanol (50%, 70%, 95%, 100%) followed by xylene, mounted in DPX solution and coverslipped.

Analysis of neuron morphology

Neurons in the dorsolateral prefrontal cortex (DLPFC, BA 46) were identified along the dorsal limb of the principal sulcus (Figure 1). Layer III pyramidal neurons were selected for

tracing and reconstruction based on the following criteria (Jacobs et al., 2001, 1997): 1) the neuron was relatively complete within a single section 2) neurons possessed well impregnated, unobscured processes with no breaks 3) somata were centrally located within the section, and 4) apical dendrites were perpendicular to the pial surface. An average of 2 neurons were traced from 5 consecutive sections (10 neurons total per case) using a computer-based neuron tracing system (Neurolucida, MicroBrightField, Williston, VT). A Zeiss microscope (Zeiss Imager Vario Z2) together with a motor stage equipped with transducers on the XYZ-axes was used to trace each neuron. Neurons were identified at low magnification (x5 objective lens), and then confirmed that they met criteria at x20 magnification before being traced at high magnification (x100 oil immersion objective lens). Apical and basal dendritic arbors were traced in their entirety. In addition to recording the depth of the soma from the pial surface, a number of morphological measures were taken including cell body size (cross section area μm^2), total length of dendrites (basal and apical, μm), number of dendritic segments (defined as a section of dendrite between branching nodes or between a branch point and the end of the dendrite (an indication of branching frequency), and spine density (number of spines per μm).

Apical dendrite trunk morphology measurements were taken from a $30\mu\text{m}$ section of primary apical dendrite located $100 \pm 10 \mu\text{m}$ from the apex of the soma. 30 neurons per case (240 neurons total) were analyzed. Criteria neurons within the chosen section were: 1) clear primary apical dendrite trunk (neurons with early bifurcation of the apical dendrite were not included) 2) no bends or kinks in the apical trunk and 3) the segment contained no oblique dendrites branch points. Measurements taken for each neuron included depth of soma from the surface, soma size (cross section area μm^2), diameter of the apical dendrite as it emerged from the soma, and the number of spines along the $30\mu\text{m}$ section. Finally, it should be noted that all data were collected with the rater blind to the treatment conditions.

Photomicrograph processing

Two-dimensional composite photomicrographs of dendritic arbors were constructed from a stacked series of images (separated by $5\mu\text{m}$) using Adobe Photoshop CS5.1 (Adobe Systems, San Jose, CA). The image in which the soma was in sharpest focus was used as a base. In-focus sections from each serial image were excised and aligned onto the base image resulting in a flattened 2-D representation of the full dendritic arbor (Figure 2A). Three-dimensional reconstructions were exported from Neurolucida and aligned in Adobe Photoshop in an overlay (Figure 2B).

Statistical analysis

All statistical analyses were performed using SPSS (version 21, IBM). 'N' was 4 per group for all analyses. Behavioral data were analyzed using the non-parametric Mann-Whitney test. Group differences in the mean for total dendritic length, segment count and spine density measured on the initial 10 cells were analyzed using a Mann-Whitney test due to non-parametric distribution. Similarly, for the apical dendrite study mean values from the 30 neurons per case were calculated followed by group mean analysis using the same statistical test. Statistical significance was set at $P < 0.05$ for all analyses.

Results

Effect of polyICLC dosing on maternal IL-6 concentration

PolyICLC injections yielded a large increase in circulating levels of interleukin-6 three hours after the injection while saline injections induced no such effect (Table 1). The 2nd polyICLC injection was associated with a more pronounced IL-6 response compared to the 6th (and final) polyICLC injection. We detected a similar trend in our larger study (see Bauman et al., 2014, Table S7) where the IL-6 response six hours after the second injection was more pronounced than the IL-6 response six hours after the third (and final) injection. However, temperature data remained consistent following multiple injections of polyICLC (see Bauman et al., 2014, Table S5) and studies in other species have not reported attenuated fever or cytokine responses following repeated polyIC injections (Soszynski et al., 1991). It is interesting to note that one of the dams that received saline injections had a low level of circulating IL-6 at the onset of the injections. We do not know if this was a low level infection or the end of a more extensive immune response. However, the neuronal morphology of the offspring from this mother was comparable to that of the other control animals.

Offspring development

There were no consistent differences across offspring in physical growth, motor or reflex development or interactions with mothers and social rearing partners. However, quantitative observations of the offspring in their home cages at approximately 6 months of age revealed that MIA-treated offspring exhibited more whole body stereotypies (i.e., pacing) compared to controls ($Z=2.31$, $P=0.029$) (Figure 3). These behaviors persisted over time (M.D. Bauman, unpublished observations) and are consistent with the emergence of repetitive behaviors described in the larger cohort of MIA-treated offspring (Bauman et al., 2014).

Analysis of neuron morphology

The effect of maternal immune activation on neuronal morphology was first evaluated by examining the morphology of the entire apical and basal dendritic arbors. Morphological measures of basal dendritic arborization (total dendritic length, spine density, segment count) of the MIA treated group were not significantly different from that of control animals (Table 2). Apical dendritic trees of the MIA treated group tended to be longer and more branched (probably due to the greater number of oblique dendrites) although this did not reach statistical significance ($P=0.08$). This is likely due to small sample size and inherent variability of neurons (Table 2 and Figure S1). Soma size (cross section area (μm^2)) did not differ between groups (Control 283.4 ± 11.4 vs. MIA 251.7 ± 22.2 ; $Z=1.16$, $P=0.248$).

In the limited 30 μm section of apical dendrite, at a distance of $100 \pm 10 \mu\text{m}$ from the soma, the apical dendrites of MIA treated animals were smaller in diameter than those of the control animals ($Z=2.31$, $P<0.05$) (Figure 4). Similar to our finding in the whole-traced neurons where there was a trend towards greater 'segment count' (an indication of branching complexity) in the MIA group, we found a significantly larger number of oblique dendrites between the soma and the beginning of the selected section ($Z=2.14$, $P<0.05$) (Figure 5). There was no difference in the number of visible spines along the 30 μm section of apical

dendrite studied (control 44.26 ± 3.2 vs. MIA 52.4 ± 3.87 ; $Z=1.73$, $P=0.08$). To correct for the spines obscured by the opaque dendrite shaft, we applied the formula outlined by Feldman and Peters (1979) (Supplemental material, Table S1). The value of N/n (where N is the 'true' number of spines calculated using the formula and n is the visible number of spines) of the control group was greater than that of the MIA group (2.5 vs. 2.35). These values represent the fact that the thicker dendrite (control group) obscures a greater number of spines, however this was not a large enough difference to drive a statistically significant difference in spine number between groups. There was also no difference in soma size (cross section area (μm^2) control 299.5 ± 7.2 vs. MIA 266.6 ± 18.7 ; $Z=1.44$, $P=0.149$).

Discussion

The present study provides the first evidence of neuropathology in rhesus macaque (*Macaca mulatta*) offspring exposed in utero to maternal immune activation (MIA). In this initial assessment of brain pathology in the nonhuman primate MIA model, dendritic morphology was quantified in layer III pyramidal neurons in dorsolateral prefrontal cortex (DLPFC, BA46) of offspring following maternal injections of the viral mimic, poly ICLC, or saline at the end of the first trimester. Our results show that MIA-treated offspring have a narrower apical dendritic diameter and a greater number of oblique dendrites compared to control offspring.

The goal of the present study was to determine if this novel, nonhuman primate model of MIA model exhibits neuropathology relevant to human neuropsychiatric diseases. We elected to focus the initial evaluation of the nonhuman primate model in the DLPFC – a region of prefrontal cortex in humans and nonhuman primates that is essential for high order cognitive processes and implicated in social cognition (Arnsten, 2011). DLPFC dysfunction is strongly implicated in SZ (Barch and Ceaser, 2012; Lesh et al., 2013; Ursu et al., 2011) and to a lesser extent ASD (Morgan et al., 2012). Analysis of post-mortem tissue from schizophrenic patients has consistently found layer III pyramidal neurons in the prefrontal cortex to have smaller somal volumes and decreased spine density compared to control cases (Glantz and Lewis, 2000; Glausier and Lewis, 2013; Kolluri et al., 2005; Pierri et al., 2001). Although neuronal morphology in DLPFC has not been specifically evaluated in postmortem ASD brains, changes in pyramidal cell morphology have been described in other cortical regions. Increased spine density was noted on the apical shaft of layer V pyramidal neurons in the mid-frontal gyrus in two out of three autistic cases (Williams et al., 1980), whereas larger studies have demonstrated regional and layer specific increases in spine density (layer II of frontal, parietal and temporal regions and in layer V of the temporal lobe (Hutsler and Zhang, 2010; Tang et al., 2014).

Although basal dendritic morphology and spine density did not differ between MIA-exposed and control offspring, we did detect a trend toward decreased somal volume in the MIA-treated animals (11.2% reduction in volume compared to control soma), which is consistent with findings in the schizophrenia literature. Moreover, in our more comprehensive assessment of apical dendrite morphology (located $100 \pm 10 \mu\text{m}$ from the soma in a $30\mu\text{m}$ section of primary apical dendrite), the apical dendrites in MIA-exposed offspring displayed distinct and consistent alterations in cell morphology. MIA-treated offspring have smaller

apical dendrite diameter and a larger number of proximal oblique dendrites than typical control offspring. Although no group differences in spine density were detected along the apical dendrite, some spines may have been obscured from view in control offspring because of the greater diameter of the apical dendrite (Feldman and Peters, 1979). Thus it was plausible that our quantification of nearly identical spine densities between MIA and control groups actually underestimated the true number of apical spines in the control offspring, thereby masking a potential decrease in spine density in MIA. To address this possible confound, we applied a correction factor outlined by Feldman and Peters (1979), however our finding of no difference in spine density remained consistent. It is also important to note that the brain tissue from the monkey MIA model was obtained during the pubescent period and thus reflects a single time point in postnatal development. Given that the majority of postmortem human neuropathology have utilized adult tissue, it is plausible that the group differences we have reported may become more pronounced with age. Likewise, the present study does not adequately address potential sex differences in MIA-treated offspring (2 males, 2 females). While gender specific differences in cognitive tasks associated with the DLPFC have been reported (Bachevalier and Hagger, 1991), there is no evidence to date of sex-related differences in dendritic morphology in layer II/III pyramidal neurons (Jacobs et al., 2001, 1993; Kolb and Stewart, 1991; Markham et al., 2013) or in androgen receptor expression in the region of interest (Finley and Kritzer, 1999).

Although our observations in the current study are from the small cohort of 8 animals used to establish dose parameters, we demonstrate a consistent finding across doses that maternal immune activation alters neuron morphology in the DLPFC. Alterations in dendritic morphology of the MIA offspring could have a critical impact on neuronal connectivity and the function of neural systems (Mainen and Sejnowski, 1996; Schaefer et al., 2003; Spruston, 2008). Although the specific mechanisms by which this may occur requires further investigation, a select number of studies may provide some insight. Interestingly, branch point morphology between oblique dendrites and the apical trunk affects signal propagation via differential impedance, thus altering neuronal activity (Ferrante et al., 2013). Layer V pyramidal neurons in rat neocortex exhibit different electrophysiological properties dependent on diameter of the apical dendrite and number of oblique dendrites (Kim and Connors, 1993). A greater number of oblique dendrites in close proximity to the soma ($<140\ \mu\text{m}$) changes the probability of action potential firing via mediation of back-propagating signals (Schaefer et al., 2003). Given the role of layer III pyramidal neurons in cortico-cortical connectivity and the importance of the DLPFC in regulation of attention, inhibition, cognitive control, motivation and emotion (Arnsten, 2011), these changes could profoundly impact behavioral development. We have previously reported that macaque offspring born to dams injected with the viral mimic polyICLC in the first trimester deviate from species-typical social development, produce motor stereotypies and self-directed behaviors, and fail to attend to salient social cues (Bauman et al., 2014; Machado et al., 2014). Although behavioral observations were not the focus of the present study, we did observe behavioral abnormalities in these MIA-treated animals that are consistent with our published reports on the second, larger MIA cohort (Bauman et al., 2014; Machado et al., 2014).

Our goal is to utilize the nonhuman primate MIA model to improve translation between rodent models and clinical populations in order to advance our understanding of the

mechanisms by which MIA during pregnancy increases the risk for human neurodevelopmental disorders. Converging evidence from rodent model suggests that activation of the maternal immune system initiates a cascade of molecular pathways that ultimately disrupt brain and behavioral development (Garay et al., 2013; Hsiao and Patterson, 2011, 2011; Patterson, 2009). The deleterious effects on brain and behavior in the mouse MIA model appear to be mediated by the maternal cytokine response, in particular interleukin (IL)-6 (Smith et al., 2007). While dams in the current study were given different doses of polyICLC to establish the most efficacious immune challenge, each of the treated dams responded with a substantial increase in IL-6 and displayed consistent alterations in cell morphology. The timing of the maternal immune challenge (early vs. late in gestation) is an important factor in the downstream effects on fetal development, and has been shown to differentially affect both behavior and neuropathology of the offspring (Fortier et al., 2007; Meyer et al., 2008, 2006). Developing fetuses in the current study were exposed to prenatal immune challenge on gestational days 43–50. In the rhesus monkey, this time coincides with the onset of neurogenesis for DLPFC and the first appearance of synapses in the marginal and subplate region of area 46 (Bourgeois et al., 1994; Levitt, 2003). Disruption of these early events associated with exposure to MIA could have long lasting effects on dendritic morphology. The postnatal timing is another important consideration given that dendritic and spine morphology in macaque monkeys undergo age-related changes (Elston et al., 2009). An important future goal is to explore the developmental progression brain pathology to determine if the MIA-induced changes in neuronal morphology are age-dependent, as has been reported following maternal LPS injection in mid-gestation in rats (Baharnoori et al., 2009).

Collectively, the nonhuman primate MIA model demonstrates that this particular prenatal immune challenge produces offspring with behavioral impairments relevant to human neurodevelopmental disorders, and brain pathology in regions implicated in these diseases. The technique of Golgi impregnation used in this study is a unique method for displaying dendritic trees of large numbers of individual neurons and has been utilized to demonstrate differences in pyramidal cell spine densities in ASD subjects compared to age-matched control cases (Hutsler and Zhang, 2010). Although more recently developed methods such as intracellular dye injections exist, they themselves are not without caveats (Hanani, 2012; Jacobs et al., 1997). While intracellular injection techniques for archived tissue are improving (Dumitriu et al., 2011), Golgi impregnation remains widely used for studying dendritic arborization and spine quantification (Bianchi et al., 2013; Jacobs et al., 2014). While the current study utilized the Golgi-cox neuron impregnation method specifically, there are multiple Golgi methods which may produce varying results (e.g., rapid Golgi vs. Golgi-cox) (Buell, 1982). Golgi-cox is an established method for non-human primate tissue with short fixation times (Morgan and Amaral, 2014). In spite of the inherent limitations in sample size associated with a nonhuman primate gestational model and the capricious nature of Golgi impregnation, significant differences were found in apical dendrite morphology in MIA exposed offspring. Moreover, these differences were consistent across varying doses. Due to these factors, the data presented here should be considered as preliminary while additional histological studies are underway to corroborate and build upon our neuropathological findings in a larger cohort of animals in a greater number of brain regions

and cortical layers. Cross-species comparisons between rodent and monkey MIA models, in addition to human studies of disorders related to MIA, will be needed to systematically evaluate the developmental progression of brain and behavior pathology following prenatal immune challenge. These results will form the basis for identifying novel preventative and therapeutic strategies aimed at alleviating the structural changes in cortical connectivity in neuroimmune-based neuropsychiatric disorders.

Supplementary Material

Refer to Web version on PubMed Central for supplementary material.

Acknowledgments

Histological studies were supported by a grant from the Brain and Behavior Research Foundation (formerly NARSAD) to M.D.B. Development of the animal model was supported by a grant from the Simons Foundation (SFARI [9900060] to P.H.P). Additional support was provided by the UC Davis RISE Award to A.K.M. and by the base grant (RR00169) of the California National Primate Research Center (CNPRC). We thank the veterinary and animal services staff of the CNPRC for care of the animals. Poly ICLC was kindly provided by Dr. Andres Salazar, MD, Oncovir, Washington D.C. We thank Dr. Bob Jacobs for his advice on Golgi quantification methodologies and for feedback on earlier drafts of this manuscript. The authors report no biomedical financial interests or potential conflicts of interest.

References

- Abdallah MW, Larsen N, Mortensen EL, Atladóttir HÓ, Nørgaard-Pedersen B, Bonefeld-Jørgensen EC, Grove J, Hougaard DM. Neonatal levels of cytokines and risk of autism spectrum disorders: an exploratory register-based historic birth cohort study utilizing the Danish Newborn Screening Biobank. *J Neuroimmunol.* 2012; 252:75–82. DOI: 10.1016/j.jneuroim.2012.07.013 [PubMed: 22917523]
- Arnsten AFT. Prefrontal cortical network connections: key site of vulnerability in stress and schizophrenia. *Int J Dev Neurosci Off J Int Soc Dev Neurosci.* 2011; 29:215–223. DOI: 10.1016/j.ijdevneu.2011.02.006
- Atladóttir HÓ, Henriksen TB, Schendel DE, Parner ET. Autism after infection, febrile episodes, and antibiotic use during pregnancy: an exploratory study. *Pediatrics.* 2012; 130:e1447–1454. DOI: 10.1542/peds.2012-1107 [PubMed: 23147969]
- Atladóttir HO, Thorsen P, Østergaard L, Schendel DE, Lemcke S, Abdallah M, Parner ET. Maternal infection requiring hospitalization during pregnancy and autism spectrum disorders. *J Autism Dev Disord.* 2010; 40:1423–1430. DOI: 10.1007/s10803-010-1006-y [PubMed: 20414802]
- Bachevalier J, Hagger C. Sex differences in the development of learning abilities in primates. *Psychoneuroendocrinology.* 1991; 16:177–188. [PubMed: 1961838]
- Baharnoori M, Brake WG, Srivastava LK. Prenatal immune challenge induces developmental changes in the morphology of pyramidal neurons of the prefrontal cortex and hippocampus in rats. *Schizophr Res.* 2009; 107:99–109. DOI: 10.1016/j.schres.2008.10.003 [PubMed: 19004618]
- Barch DM, Ceaser A. Cognition in schizophrenia: core psychological and neural mechanisms. *Trends Cogn Sci.* 2012; 16:27–34. DOI: 10.1016/j.tics.2011.11.015 [PubMed: 22169777]
- Bauman MD, Iosif AM, Smith SEP, Bregere C, Amaral DG, Patterson PH. Activation of the maternal immune system during pregnancy alters behavioral development of rhesus monkey offspring. *Biol Psychiatry.* 2014; 75:332–341. DOI: 10.1016/j.biopsych.2013.06.025 [PubMed: 24011823]
- Bianchi S, Stimpson CD, Duka T, Larsen MD, Janssen WGM, Collins Z, Bauernfeind AL, Schapiro SJ, Baze WB, McArthur MJ, Hopkins WD, Wildman DE, Lipovich L, Kuzawa CW, Jacobs B, Hof PR, Sherwood CC. Synaptogenesis and development of pyramidal neuron dendritic morphology in the chimpanzee neocortex resembles humans. *Proc Natl Acad Sci U S A.* 2013; 110(Suppl 2): 10395–10401. DOI: 10.1073/pnas.1301224110 [PubMed: 23754422]

- Boks P. Effects of prenatal infection on brain development and behavior: a review of findings from animal models. *Brain Behav Immun*. 2010; 24:881–897. DOI: 10.1016/j.bbi.2010.03.005 [PubMed: 20230889]
- Bourgeois JP, Goldman-Rakic PS, Rakic P. Synaptogenesis in the prefrontal cortex of rhesus monkeys. *Cereb Cortex N Y N* 1991. 1994; 4:78–96.
- Brown AS, Begg MD, Gravenstein S, Schaefer CA, Wyatt RJ, Bresnahan M, Babulas VP, Susser ES. Serologic evidence of prenatal influenza in the etiology of schizophrenia. *Arch Gen Psychiatry*. 2004; 61:774–780. DOI: 10.1001/archpsyc.61.8.774 [PubMed: 15289276]
- Buell SJ. Golgi-Cox and rapid golgi methods as applied to autopsied human brain tissue: widely disparate results. *J Neuropathol Exp Neurol*. 1982; 41:500–507. [PubMed: 6180137]
- Caskey M, Lefebvre F, Filali-Mouhim A, Cameron MJ, Goulet JP, Haddad EK, Breton G, Trumpfheller C, Pollak S, Shimeliovich I, Duque-Alarcon A, Pan L, Nelkenbaum A, Salazar AM, Schlesinger SJ, Steinman RM, Sékaly RP. Synthetic double-stranded RNA induces innate immune responses similar to a live viral vaccine in humans. *J Exp Med*. 2011; 208:2357–2366. DOI: 10.1084/jem.20111171 [PubMed: 22065672]
- Das G, Reuhl K, Zhou R. The Golgi-Cox method. *Methods Mol Biol Clifton NJ*. 2013; 1018:313–321. DOI: 10.1007/978-1-62703-444-9_29
- De Clercq E. Degradation of poly(inosinic acid) - poly(cytidylic acid) [(I)n - (C)n] by human plasma. *Eur J Biochem FEBS*. 1979; 93:165–172.
- Dumitriu D, Rodriguez A, Morrison JH. High-throughput, detailed, cell-specific neuroanatomy of dendritic spines using microinjection and confocal microscopy. *Nat Protoc*. 2011; 6:1391–1411. DOI: 10.1038/nprot.2011.389 [PubMed: 21886104]
- Elston GN, Oga T, Fujita I. Spinogenesis and pruning scales across functional hierarchies. *J Neurosci Off J Soc Neurosci*. 2009; 29:3271–3275. DOI: 10.1523/JNEUROSCI.5216-08.2009
- Fatemi SH, Reutiman TJ, Folsom TD, Huang H, Oishi K, Mori S, Smee DF, Pearce DA, Winter C, Sohr R, Juckel G. Maternal infection leads to abnormal gene regulation and brain atrophy in mouse offspring: implications for genesis of neurodevelopmental disorders. *Schizophr Res*. 2008; 99:56–70. DOI: 10.1016/j.schres.2007.11.018 [PubMed: 18248790]
- Feldman ML, Peters A. A technique for estimating total spine numbers on Golgi-impregnated dendrites. *J Comp Neurol*. 1979; 188:527–542. DOI: 10.1002/cne.901880403 [PubMed: 93115]
- Ferrante M, Migliore M, Ascoli GA. Functional impact of dendritic branch-point morphology. *J Neurosci Off J Soc Neurosci*. 2013; 33:2156–2165. DOI: 10.1523/JNEUROSCI.3495-12.2013
- Finley SK, Kritzer MF. Immunoreactivity for intracellular androgen receptors in identified subpopulations of neurons, astrocytes and oligodendrocytes in primate prefrontal cortex. *J Neurobiol*. 1999; 40:446–457. [PubMed: 10453048]
- Fortier ME, Luheshi GN, Boks P. Effects of prenatal infection on prepulse inhibition in the rat depend on the nature of the infectious agent and the stage of pregnancy. *Behav Brain Res*. 2007; 181:270–277. DOI: 10.1016/j.bbr.2007.04.016 [PubMed: 17553574]
- Garay PA, Hsiao EY, Patterson PH, McAllister AK. Maternal immune activation causes age- and region-specific changes in brain cytokines in offspring throughout development. *Brain Behav Immun*. 2013; 31:54–68. DOI: 10.1016/j.bbi.2012.07.008 [PubMed: 22841693]
- Glantz LA, Lewis DA. Decreased dendritic spine density on prefrontal cortical pyramidal neurons in schizophrenia. *Arch Gen Psychiatry*. 2000; 57:65–73. [PubMed: 10632234]
- Glaser EM, Van der Loos H. Analysis of thick brain sections by obverse-reverse computer microscopy: application of a new, high clarity Golgi-Nissl stain. *J Neurosci Methods*. 1981; 4:117–125. [PubMed: 6168870]
- Glausier JR, Lewis DA. Dendritic spine pathology in schizophrenia. *Neuroscience*. 2013; 251:90–107. DOI: 10.1016/j.neuroscience.2012.04.044 [PubMed: 22546337]
- Hanani M. Lucifer yellow - an angel rather than the devil. *J Cell Mol Med*. 2012; 16:22–31. DOI: 10.1111/j.1582-4934.2011.01378.x [PubMed: 21740513]
- Hsiao EY, Patterson PH. Activation of the maternal immune system induces endocrine changes in the placenta via IL-6. *Brain Behav Immun*. 2011; 25:604–615. DOI: 10.1016/j.bbi.2010.12.017 [PubMed: 21195166]

- Hutsler JJ, Zhang H. Increased dendritic spine densities on cortical projection neurons in autism spectrum disorders. *Brain Res.* 2010; 1309:83–94. DOI: 10.1016/j.brainres.2009.09.120 [PubMed: 19896929]
- Jacobs B, Driscoll L, Schall M. Life-span dendritic and spine changes in areas 10 and 18 of human cortex: a quantitative Golgi study. *J Comp Neurol.* 1997; 386:661–680. [PubMed: 9378859]
- Jacobs B, Johnson NL, Wahl D, Schall M, Maseko BC, Lewandowski A, Raghanti MA, Wicinski B, Butti C, Hopkins WD, Bertelsen MF, Walsh T, Roberts JR, Reep RL, Hof PR, Sherwood CC, Manger PR. Comparative neuronal morphology of the cerebellar cortex in afrotherians, carnivores, cetartiodactyls, and primates. *Front Neuroanat.* 2014; 8:24.doi: 10.3389/fnana.2014.00024 [PubMed: 24795574]
- Jacobs B, Schall M, Prather M, Kapler E, Driscoll L, Baca S, Jacobs J, Ford K, Wainwright M, Trembl M. Regional dendritic and spine variation in human cerebral cortex: a quantitative golgi study. *Cereb Cortex N Y N 1991.* 2001; 11:558–571.
- Jacobs B, Schall M, Scheibel AB. A quantitative dendritic analysis of Wernicke's area in humans. II Gender, hemispheric, and environmental factors. *J Comp Neurol.* 1993; 327:97–111. DOI: 10.1002/cne.903270108 [PubMed: 8432910]
- Kim HG, Connors BW. Apical dendrites of the neocortex: correlation between sodium- and calcium-dependent spiking and pyramidal cell morphology. *J Neurosci Off J Soc Neurosci.* 1993; 13:5301–5311.
- Kolb B, Stewart J. Sex-related differences in dendritic branching of cells in the prefrontal cortex of rats. *J Neuroendocrinol.* 1991; 3:95–99. DOI: 10.1111/j.1365-2826.1991.tb00245.x [PubMed: 19215453]
- Kolluri N, Sun Z, Sampson AR, Lewis DA. Lamina-specific reductions in dendritic spine density in the prefrontal cortex of subjects with schizophrenia. *Am J Psychiatry.* 2005; 162:1200–1202. DOI: 10.1176/appi.ajp.162.6.1200 [PubMed: 15930070]
- Lee BK, Magnusson C, Gardner RM, Blomström S, Newschaffer CJ, Burstyn I, Karlsson H, Dalman C. Maternal hospitalization with infection during pregnancy and risk of autism spectrum disorders. *Brain Behav Immun.* 2014; doi: 10.1016/j.bbi.2014.09.001
- Lesh TA, Westphal AJ, Niendam TA, Yoon JH, Minzenberg MJ, Ragland JD, Solomon M, Carter CS. Proactive and reactive cognitive control and dorsolateral prefrontal cortex dysfunction in first episode schizophrenia. *NeuroImage Clin.* 2013; 2:590–599. DOI: 10.1016/j.nicl.2013.04.010 [PubMed: 24179809]
- Levitt P. Structural and functional maturation of the developing primate brain. *J Pediatr.* 2003; 143:S35–45. [PubMed: 14597912]
- Levy HB, Baer G, Baron S, Buckler CE, Gibbs CJ, Iadarola MJ, London WT, Rice J. A modified polyribonucleoside-polyribocytidylic acid complex that induces interferon in primates. *J Infect Dis.* 1975; 132:434–439. [PubMed: 810520]
- Machado CJ, Whitaker AM, Smith SEP, Patterson PH, Bauman MD. Maternal Immune Activation in Nonhuman Primates Alters Social Attention in Juvenile Offspring. *Biol Psychiatry.* 2014; doi: 10.1016/j.biopsych.2014.07.035
- Mainen ZF, Sejnowski TJ. Influence of dendritic structure on firing pattern in model neocortical neurons. *Nature.* 1996; 382:363–366. DOI: 10.1038/382363a0 [PubMed: 8684467]
- Malkova NV, Yu CZ, Hsiao EY, Moore MJ, Patterson PH. Maternal immune activation yields offspring displaying mouse versions of the three core symptoms of autism. *Brain Behav Immun.* 2012; 26:607–616. DOI: 10.1016/j.bbi.2012.01.011 [PubMed: 22310922]
- Markham JA, Mullins SE, Koenig JI. Periadolescent maturation of the prefrontal cortex is sex-specific and is disrupted by prenatal stress. *J Comp Neurol.* 2013; 521:1828–1843. DOI: 10.1002/cne.23262 [PubMed: 23172080]
- Matsumoto M, Seya T. TLR3: interferon induction by double-stranded RNA including poly(I:C). *Adv Drug Deliv Rev.* 2008; 60:805–812. DOI: 10.1016/j.addr.2007.11.005 [PubMed: 18262679]
- Mednick SA, Machon RA, Huttunen MO, Bonett D. Adult schizophrenia following prenatal exposure to an influenza epidemic. *Arch Gen Psychiatry.* 1988; 45:189–192. [PubMed: 3337616]
- Meyer U, Nyffeler M, Engler A, Urwyler A, Schedlowski M, Knuesel I, Yee BK, Feldon J. The time of prenatal immune challenge determines the specificity of inflammation-mediated brain and

- behavioral pathology. *J Neurosci Off J Soc Neurosci*. 2006; 26:4752–4762. DOI: 10.1523/JNEUROSCI.0099-06.2006
- Meyer U, Nyffeler M, Yee BK, Knuesel I, Feldon J. Adult brain and behavioral pathological markers of prenatal immune challenge during early/middle and late fetal development in mice. *Brain Behav Immun*. 2008; 22:469–486. DOI: 10.1016/j.bbi.2007.09.012 [PubMed: 18023140]
- Morgan JT, Amaral DG. Comparative analysis of the dendritic organization of principal neurons in the lateral and central nuclei of the rhesus macaque and rat amygdala. *J Comp Neurol*. 2014; 522:689–716. DOI: 10.1002/cne.23467 [PubMed: 24114951]
- Morgan JT, Chana G, Abramson I, Semendeferi K, Courchesne E, Everall IP. Abnormal microglial-neuronal spatial organization in the dorsolateral prefrontal cortex in autism. *Brain Res*. 2012; 1456:72–81. DOI: 10.1016/j.brainres.2012.03.036 [PubMed: 22516109]
- Nordlund JJ, Wolff SM, Levy HB. Inhibition of biologic activity of poly I: poly C by human plasma. *Proc Soc Exp Biol Med Soc Exp Biol Med N Y N*. 1970; 133:439–444.
- Patterson PH. Immune involvement in schizophrenia and autism: etiology, pathology and animal models. *Behav Brain Res*. 2009; 204:313–321. DOI: 10.1016/j.bbr.2008.12.016 [PubMed: 19136031]
- Pierri JN, Volk CL, Auh S, Sampson A, Lewis DA. Decreased somal size of deep layer 3 pyramidal neurons in the prefrontal cortex of subjects with schizophrenia. *Arch Gen Psychiatry*. 2001; 58:466–473. [PubMed: 11343526]
- Piontkewitz Y, Arad M, Weiner I. Tracing the development of psychosis and its prevention: what can be learned from animal models. *Neuropharmacology*. 2012; 62:1273–1289. DOI: 10.1016/j.neuropharm.2011.04.019 [PubMed: 21703648]
- Rosoklija G, Mancevski B, Ilievski B, Perera T, Lisanby SH, Coplan JD, Duma A, Serafimova T, Dwork AJ. Optimization of Golgi methods for impregnation of brain tissue from humans and monkeys. *J Neurosci Methods*. 2003; 131:1–7. [PubMed: 14659818]
- Schaefer AT, Larkum ME, Sakmann B, Roth A. Coincidence detection in pyramidal neurons is tuned by their dendritic branching pattern. *J Neurophysiol*. 2003; 89:3143–3154. DOI: 10.1152/jn.00046.2003 [PubMed: 12612010]
- Shi L, Fatemi SH, Sidwell RW, Patterson PH. Maternal influenza infection causes marked behavioral and pharmacological changes in the offspring. *J Neurosci Off J Soc Neurosci*. 2003; 23:297–302.
- Short SJ, Lubach GR, Karasin AI, Olsen CW, Styner M, Knickmeyer RC, Gilmore JH, Coe CL. Maternal influenza infection during pregnancy impacts postnatal brain development in the rhesus monkey. *Biol Psychiatry*. 2010; 67:965–973. DOI: 10.1016/j.biopsych.2009.11.026 [PubMed: 20079486]
- Smith SEP, Li J, Garbett K, Mirnics K, Patterson PH. Maternal immune activation alters fetal brain development through interleukin-6. *J Neurosci Off J Soc Neurosci*. 2007; 27:10695–10702. DOI: 10.1523/JNEUROSCI.2178-07.2007
- Sørensen HJ, Mortensen EL, Reinisch JM, Mednick SA. Association between prenatal exposure to bacterial infection and risk of schizophrenia. *Schizophr Bull*. 2009; 35:631–637. DOI: 10.1093/schbul/sbn121 [PubMed: 18832344]
- Soszynski D, Kozak W, Szewczenko M. Course of fever response to repeated administration of sublethal doses of lipopolysaccharides, polyinosinic:polycytidylic acid and muramyl dipeptide to rabbits. *Experientia*. 1991; 47:43–47. [PubMed: 1999244]
- Spruston N. Pyramidal neurons: dendritic structure and synaptic integration. *Nat Rev Neurosci*. 2008; 9:206–221. DOI: 10.1038/nrn2286 [PubMed: 18270515]
- Tang G, Gudsnek K, Kuo SH, Cotrina ML, Rosoklija G, Sosunov A, Sonders MS, Kanter E, Castagna C, Yamamoto A, Yue Z, Arancio O, Peterson BS, Champagne F, Dwork AJ, Goldman J, Sulzer D. Loss of mTOR-dependent macroautophagy causes autistic-like synaptic pruning deficits. *Neuron*. 2014; 83:1131–1143. DOI: 10.1016/j.neuron.2014.07.040 [PubMed: 25155956]
- Ursu S, Kring AM, Gard MG, Minzenberg MJ, Yoon JH, Ragland JD, Solomon M, Carter CS. Prefrontal cortical deficits and impaired cognition-emotion interactions in schizophrenia. *Am J Psychiatry*. 2011; 168:276–285. DOI: 10.1176/appi.ajp.2010.09081215 [PubMed: 21205806]

- Watson KK, Platt ML. Of mice and monkeys: using non-human primate models to bridge mouse- and human-based investigations of autism spectrum disorders. *J Neurodev Disord*. 2012; 4:21.doi: 10.1186/1866-1955-4-21 [PubMed: 22958282]
- Willette AA, Lubach GR, Knickmeyer RC, Short SJ, Styner M, Gilmore JH, Coe CL. Brain enlargement and increased behavioral and cytokine reactivity in infant monkeys following acute prenatal endotoxemia. *Behav Brain Res*. 2011; 219:108–115. DOI: 10.1016/j.bbr.2010.12.023 [PubMed: 21192986]
- Williams RS, Hauser SL, Purpura DP, DeLong GR, Swisher CN. Autism and mental retardation: neuropathologic studies performed in four retarded persons with autistic behavior. *Arch Neurol*. 1980; 37:749–753. [PubMed: 7447762]
- Zuckerman L, Weiner I. Post-pubertal emergence of disrupted latent inhibition following prenatal immune activation. *Psychopharmacology (Berl)*. 2003; 169:308–313. DOI: 10.1007/s00213-003-1461-7 [PubMed: 12748757]
- Zuckerman L, Weiner I. Maternal immune activation leads to behavioral and pharmacological changes in the adult offspring. *J Psychiatr Res*. 2005; 39:311–323. DOI: 10.1016/j.jpsychires.2004.08.008 [PubMed: 15725430]

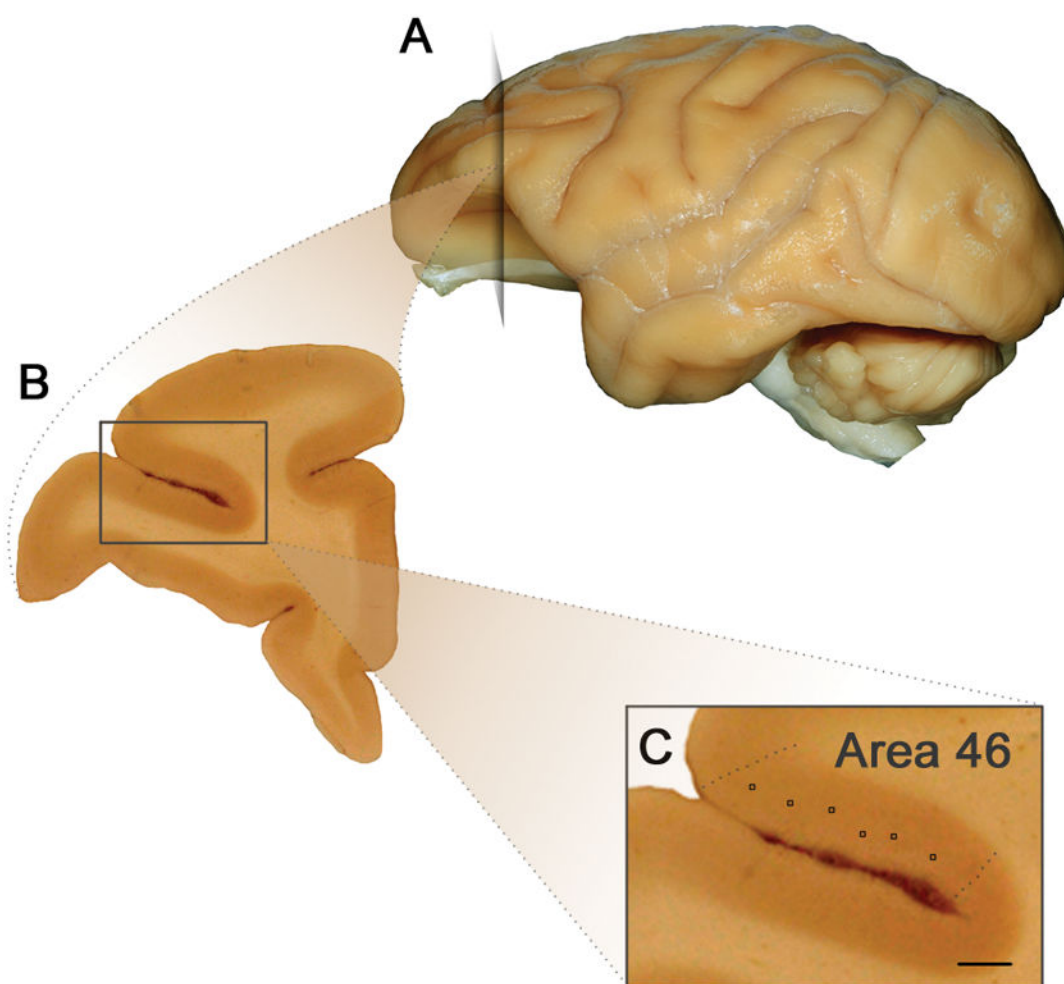


Figure 1. Neuroanatomy of dorsolateral prefrontal cortex. A) Lateral view of the left hemisphere indicating location of the coronal section depicted in B). B) Coronal section through DLPFC C) Approximate position of layer III pyramidal neuron soma measured along the dorsal limb of the principal sulcus (scale bar = 0.8mm).

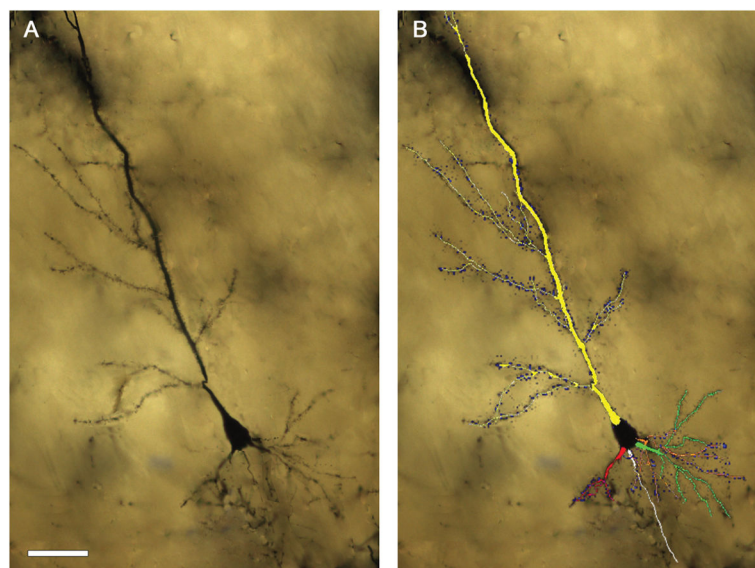


Figure 2.

A) Example of a Golgi impregnated layer III pyramidal neuron B) the same neuron with overlaid 3-D reconstruction of dendritic arbors from Neurolucida. Apical dendrite (yellow), basal dendrites (green, orange and red), axon (white) and spines (blue). Scale bar = 50 μ m

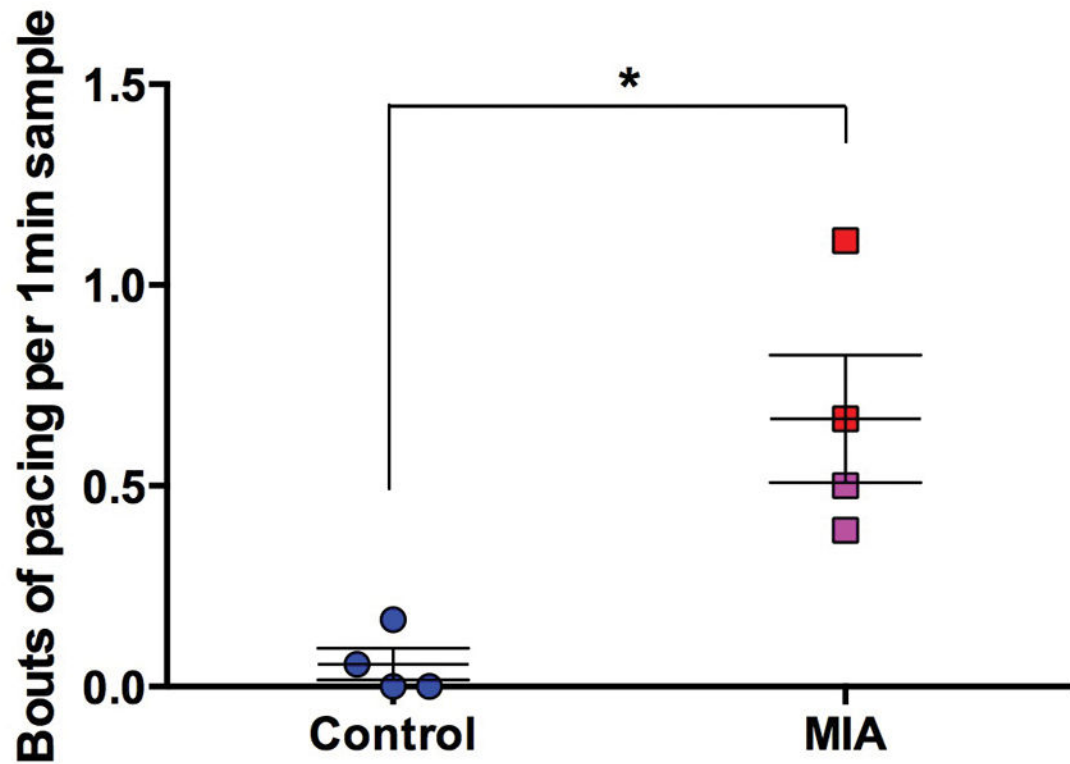


Figure 3.

MIA treated animals exhibited more whole body stereotypies (i.e., pacing) compared to saline treated controls at 6 months of age. Each animal underwent 18 home cage observations (9 morning and 9 afternoon) comprising of six 10-second periods. Individual behaviors were scored using a one-zero sampling method corresponding to presence or absence of the behavior respectively (therefore the maximum score of any behavior over a single observation was 6). Scores were averaged across the 18 observations. (Control animals (all male – (blue)), MIA males (red), MIA female animals (pink), *P<0.05)

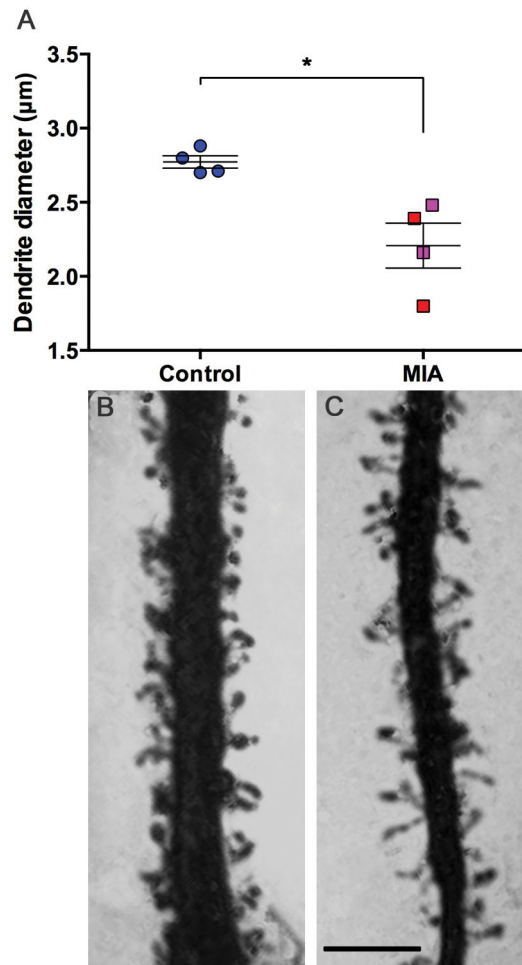


Figure 4.

Diameter (μm) of apical dendrite shaft. MIA animals have thinner apical dendrites than control animals (A). Representative photomicrographs of control (B) and MIA (C) apical dendrites. (Control animals (all male – (blue)), MIA males (red), MIA female animals (pink)), scale bar = 5μm, *P<0.05)

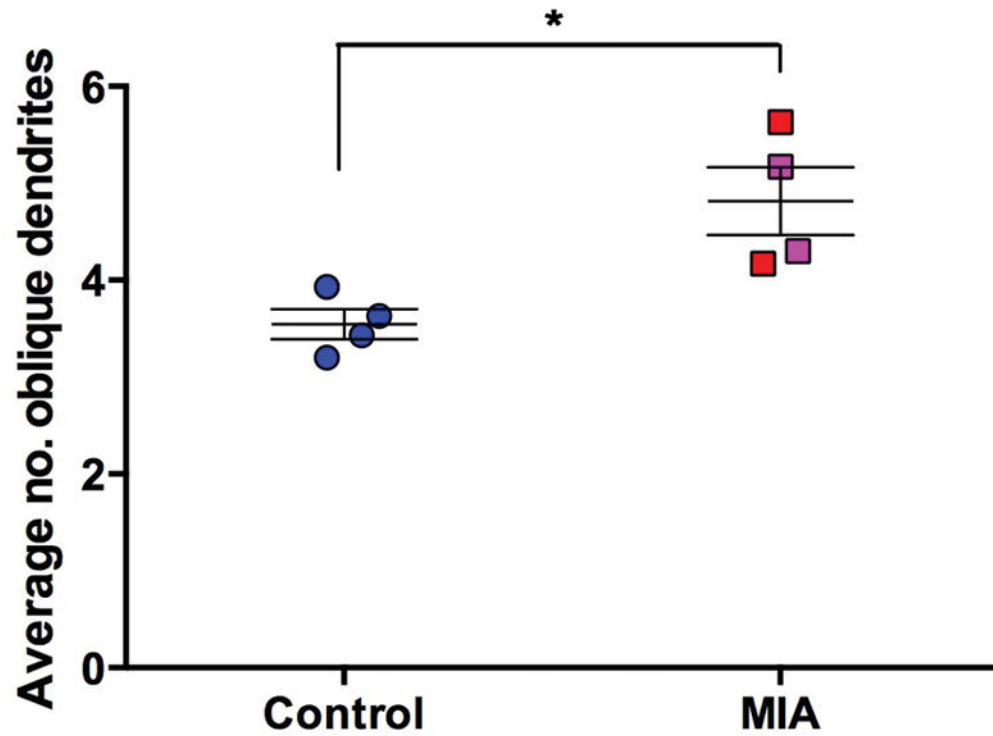


Figure 5.

Average number of oblique dendrites within the first 100µm of apical dendrite. MIA animals have a greater number of proximal dendrites compared to control animals. (Control animals (all male – (blue)), MIA males (red), MIA female animals (pink), * $P < 0.05$)

Table 1

Experimental groups and maternal response to polyICLC

Treatment (dose mg/kg)	Baseline IL-6 (pg/ml)	IL-6 – 3 hr after first polyICLC injection (pg/ml)	IL-6 – 3 hr after final polyICLC injection (pg/ml)	Offspring gender	Age of offspring at sacrifice (Months)
Saline	0	0	0	Male	41
Saline	0	0	0	Male	41
Saline	0	0	0	Male	43
Saline	60	55.3	38.6	Male	46
PolyICLC (0.25)	0	3635.0	324.4	Female	41
PolyICLC (0.5)	0	6938.2	155.0	Female	42
PolyICLC (0.5)	0	14302.0	3789.8	Male	46
PolyICLC (1.0)	0	23441.0	1200.0	Male	44

Summary data of apical and basal morphological measures (group mean averages compiled from 10 cells per case). No significant group differences were found.

Table 2

		Control		MIA	
		Mean	SEM	Mean	SEM
Apical dendrites	Total length (µm)	1162.3	(145.20)	1415.5	(93.83)
	Spine density (spines per µm)	0.80	(0.04)	0.79	(0.02)
	Segment count	22.5	(2.81)	29.20	(1.40)
Basal dendrites	Total length (µm)	1478.72	(164.10)	1378.0	(109.21)
	Spine density (spines per µm)	0.76	(0.05)	0.74	(0.01)
	Segment count	34.74	(3.53)	35.5	(1.82)